REVIEW

Surface-enhanced Raman spectroscopy: substrate-related issues

Xiu-Mei Lin · Yan Cui · Yan-Hui Xu · Bin Ren ·
Zhong-Qun Tian

Abstract After over 30 years of development, surface-enhanced Raman spectroscopy (SERS) is now facing a very important stage in its history. The explosive development of nanoscience and nanotechnology has assisted the rapid development of SERS, especially during the last 5 years. Further development of surface-enhanced Raman spectroscopy is mainly limited by the reproducible preparation of clean and highly surface enhanced Raman scattering (SERS) active substrates. This review deals with some substrate-related issues. Various methods will be introduced for preparing SERS substrates of Ag and Au for analytical purposes, from SERS substrates prepared by electrochemical or vacuum methods, to well-dispersed Au or Ag nanoparticle sols, to nanoparticle thin film substrates, and finally to ordered nanostructured substrates. Emphasis is placed on the analysis of the advantages and weaknesses of different methods in preparing SERS substrates. Closely related to the application of SERS in the analysis of trace sample and unknown systems, the existing cleaning methods for SERS substrates are analyzed and a combined chemical adsorption and electrochemical oxidation method is proposed to eliminate the interference of contaminants. A defocusing method is proposed to deal with the laser-induced sample decomposition problem frequently met in SERS measurement to obtain strong signals. The existing methods to estimate the surface enhancement factor, a criterion to characterize the SERS activity of a substrate, are analyzed and some guidelines are proposed to obtain the correct enhancement factor.

Keywords Silver · Gold · Substrate preparation · Substrate cleaning · Photodecomposition · Surface enhancement factor

X.-M. Lin · Y. Cui · B. Ren (✉) · Z.-Q. Tian
State Key Laboratory for Physical Chemistry of Solid Surfaces
and Department of Chemistry,
College of Chemistry and Chemical Engineering,
Xiamen University,
Xiamen 361005, China
e-mail: bren@xmu.edu.cn

Y.-H. Xu
Research Center of Biomedical Engineering, College of Materials,
Xiamen University,
Xiamen 361005, China

Introduction

Raman spectroscopy is capable of obtaining fingerprint information of species by detecting the vibrational bands. However, the Raman signal of most systems is very weak and is only about 10^{-10} times the intensity of the incident laser [1, 2]. The signal becomes even weaker when the adsorbed species are concerned, because there are only monolayer or submonolayer species on the surface. In Raman measurements other than in a pure liquid or solid, a certain kind of enhancement effect should be employed to boost the signal, such as the resonance Raman effect, the surface enhanced Raman scattering (SERS) effect [3], or the tip-enhanced Raman effect [4]. The first observation of surface-enhanced Raman spectra was in 1974, when Fleischmann et al. [5] reported the first high-quality Raman spectra of monolayer-adsorbed pyridine on an electrochemically roughened Ag electrode surface. Three years later, the Van Duyne group [6] and the Creighton group [7]

independently pointed out that the million-fold enhancement is due to a kind of surface enhancement effect. These exciting early observations have stimulated intensive experimental and theoretical works and SERS has found wide application in surface sciences, analytical sciences, biological sciences, etc. [8–10].

Meanwhile, the investigation of the SERS mechanisms has never stopped. It is now widely accepted that electromagnetic enhancement and chemical enhancement are the two major enhancement mechanisms contributing to the giant SERS, with the former being the dominant contribution [11–13]. The chemical enhancement mechanism reflects the enhancement as a result of the chemical interaction between the adsorbates and the metal surface. Among the various types of chemical enhancements, including chemical bonding enhancement, resonance enhancement of a surface complex, and photon-induced charge-transfer enhancement (PICT) [14, 15], PICT is the most important. It describes the optical resonance excitation of the charge-transfer state formed by the surface complex of the metal adatom and the adsorbate [16–18]. Chemical enhancement is a short-range effect occurring in the range of molecular scale. Electromagnetic enhancement comes from the interaction of light (both incident and scattered) with the substrate. It is a long-range effect not depending on the properties of the probe molecules. Localized surface plasmon resonance (LSPR), the lightning rod effect, and the image field effect have all been considered to contribute to SERS [19, 20]. Among them, LSPR makes the major contribution to the electromagnetic field enhancement and therefore SERS. The LSPR strength and frequency are influenced by the incident laser wavelength, the morphology of the substrate, and the surrounding medium. By controlling the composition, shape, size, and the interparticle spacing of nanoparticles and their assemblies, one can tune the LSPR to obtain the optimized SERS substrate at the desired wavelength [21, 22].

However, whether SERS can achieve a broader application really depends on the SERS activity and the reproducibility of the substrate [23]. Ever since the first observation of SERS on an electrochemically roughened Ag electrode, the preparation methods of SERS substrates have gone through the following stages: (1) random and nonuniform substrates prepared by electrochemical oxidation and reduction cycles(s) (EC-ORC) or vacuum deposition methods; (2) nanoparticle sols with a large size distribution prepared by wet chemical synthesis or a laser ablation method; (3) nanoparticles with controlled size and shape prepared by a chemical synthesis method; and (4) large-area surface nanostructures with defined size, shape, and interparticle spacing prepared by self-assembly, template, or lithography methods. Especially, in the last 15 years, the preparation of SERS substrates has become more controllable, benefiting from the development of nanoscience and nanotechnology. As a result, SERS has found a further application in quantitative analysis [24–26], trace analysis [27–29], and the analysis of bio-related systems [30–32].

Combining the concluding remark made by Natan [23] at Faraday Discussion 132, we can easily outline the features of an ideal SERS substrate:

1. The substrate should have high SERS activity and therefore provide high sensitivity. By controlling the size (more than 50 nm) and interparticle spacing (less than 10 nm) of nanoparticles, one can tune the LSPR frequency of the substrate to match the incident laser frequency and the effective coupling between nanoparticles can be induced to maximize the enhancement.
2. The substrate should be uniform so that the deviation in enhancement over the whole surface can be less than 20%, which requires a relatively ordered arrangement of the nanoparticles on the substrate.
3. The substrate should have good stability and reproducibility. Even after a long shelf time, the enhancement effect can still be maintained. The deviation in the enhancement should be less than 20% for different batches of substrates prepared by the same method.
4. The substrate should be clean enough so that it can be applied to study not only strong adsorbates but also some weak adsorbates or even unknown samples.

Unfortunately, at present, it is still difficult to obtain SERS substrates that can simultaneously meet all of the above requirements. According to the specific application purpose, one has to make some trade-offs. For example, in quantitative analysis, a uniform and reproducible substrate is extremely important; however, in trace analysis, the maximized enhancement is the prerequisite. In bio-related detection, a clean and highly enhanced substrate is generally required owing to the complexity in biosystems studied to allow for a reasonable assignment of the detected spectral bands.

In the present critical review, we will firstly introduce various methods to prepare SERS substrates. We have introduced this aspect in several of our previous reviews [33, 34], and the focus of present review will be on the preparation of metal nanoparticles and highly ordered SERS substrates and the advantages and challenges when they are used as SERS substrates. We will then deal with the issue of contaminants frequently met in SERS, especially in SERS analysis of trace sample and unknown systems. A method will be proposed to handle the laser-induced decomposition problem frequently met in SERS measurement with a confocal micro Raman instrument. Finally, we will show how to correctly calculate the surface enhancement factor.

Methods for preparing SERS substrates

EC-ORC and vacuum deposition methods

The first SERS spectra were obtained on a rough Ag surface prepared by EC-ORC [5]. By application of an oxidation potential to the metal electrode, the electrode will be oxidized to soluble compounds or will form a surface complex. A reduction potential will then reduce these dissolved species on the surface, forming surface nanostructures. To ensure reproducibility, the metal surfaces should first be mechanically polished, ultrasonically cleaned to obtain a clean surface, and then roughened in certain electrolytes (KCl or H_2SO_4) with a special waveform of potential or current control to allow the oxidation and reduction of the surface [33]. Using this method, we can easily obtain SERS-active Ag and Cu surfaces. For the Au surface, special care has to be taken regarding the waveform applied and the cleanliness of the surface [35]. The common enhancement achieved using this method can be as high as 10^4–10^6 for Ag, Au, and Cu, and 10^1–10^4 for other transition metal substrates, such as Fe, Co, Ni, Rh, Pd, and Pt [36]. EC-ORC is a very simple method for preparing a SERS substrate with very good stability. It has less chance of being contaminated. With such a conductive substrate, potential-dependent SERS measurement can be performed to study the SERS mechanism, especially the chemical enhancement mechanism. Such a substrate has a random surface structure formed by nanoparticles with a wide size and shape distribution. Therefore, different areas of the surface may have quite different enhancements. As common practice, one has to check the surface to find the most representative spots for a series of Raman measurements to ensure the reproducibility of the SERS experiment [33, 36]. To obtain a higher enhancement on the transition metal surface for studying the surface adsorbates, a very thin layer (several atomic layers to several tens of atomic layers) of transition metals (Pt group metal) has been deposited on highly SERS active Ag or Au surfaces by electrochemical methods to utilize the long-range effect of SERS [37, 38]. The method has been used to study the adsorption and reaction of molecules on the transition metal surfaces and has provided a wealth of meaningful data and conclusions for understanding the electrochemical interfaces and the electrocatalytic processes [39]. It should be pointed out that the influence of the substrate metal on the physical and chemical properties of overlayer metals and the stability and the reversibility of the thin layer still limit a wider application of the method. To overcome these problems, our group used core–shell nanoparticle methods to obtain SERS substrates of transition metals with a high enhancement, which will be discussed in detail later. In parallel to EC-ORC, those laboratories equipped with a vacuum deposition system tend to use vacuum deposition methods to prepare SERS substrates. The main purpose is to form a rough metal film or discontinuous metal islands in the vacuum chamber by depositing metal atoms on the substrates, which can be a Si wafer, a glass slide, graphite, or a mechanically polished rough substrate or even nanostructured substrates [40–44]. By controlling the temperature of the substrate and the deposition rate during the deposition process, one can obtain metal films with different SERS activity. For example, if the metal vapor is deposited on a cold substrate (typically lower than 120 K), a rough metal film will be obtained. With increase of the temperature, the migration of the metal atoms will be accelerated, leading to the formation of an island-like structure.

Both EC-ORC and vacuum deposition methods have difficultly to produce very uniform structures; therefore, different points may have different enhancement effects. Furthermore, both methods need specialized equipment, such as a potentiostat or a vacuum deposition system. Which of the two methods is selected really depends on the instrumentation available in the laboratory. To overcome these problems, nanoassembly or nanolithography methods have been used to fabricate ordered substrates, followed by vacuum deposition or electrochemical methods to produce comparably ordered substrates, which will be discussed further later.

Chemical synthesis for producing well-dispersed nanoparticles

With the vast development of nanoscience and nanotechnology, metal nanoparticles of different sizes and shapes have been synthesized using various methods, such as chemical reduction, chemical replacement, electrochemical reduction, photochemical, thermal decomposition, and ultrasonic decomposition methods [45]. The simplest and the most widely used method is the chemical reduction method, in which a metal salt is reduced to metal nanoparticles in aqueous or nonaqueous solution by reductants, such as sodium citrate [46], $NaBH_4$ [47], hydrogen [48], or alcohols [49]. Normally some surfactants, such as cetyl trimethylammonium bromide (CTAB), poly (vinyl pyrrolidone) (PVP), or sodium dodecyl sulfate ($C_{12}H_{25}SO_3Na$), are be added to the solution as capping agents to prevent the aggregation or oxidation of the synthesized nanoparticles or to adjust the growth rate of different facets to control the shape and size of the nanoparticles. The type of metal salt, reductant, surfactant, and their relative concentration, the reaction temperature, and the solution pH all influence the size and size

distribution, the shape, and the aggregation state of particles. For example, in the presence of CTAB and at a high ascorbic acid concentration, spherical Au seeds will grow into Au nanocubes (Fig. 1a). If only the concentration of the Au seeds is increased, the nanocubes will be transformed into nanotriangles (Fig. 1b). If the concentrations of the Au seeds, CTAB, and Au^{3+} are increased, the nanocubes will be transformed into tetrapods (Fig. 1c). The variation of the seed-to-Au^{3+} concentration ratio and the concentrations of CTAB and ascorbic acid will result in a shape transformation from a tetrapod to a star (Fig. 1d) [50]. Owing to the unique optical properties, most Au, Ag, and Cu nanoparticles (sphere, rod, cube, or triangle) have more or less strong SERS activity and other transition metal (such as Pt group or Fe group metals) nanoparticles have weaker SERS activity. SERS-active nanoparticles can be of monometallic, alloy, or bimetallic composition. They can be used as SERS substrates in the form of well-dispersed nanoparticles, nanoparticle aggregates, or even multilayer nanoparticle thin films. In comparison with EC-ORC or vacuum deposition methods, the use of metal nanoparticles as SERS substrates may have the following advantages: (1) easy to synthesize at a low cost; (2) the size and shape can be controlled by reaction conditions to obtain the desired optical properties and the maximized enhancement effect; (3) the aggregated nanoparticles can provide very high enhancement up to single-molecule sensitivity [51, 52].

Since the first application of Ag and Au sols as SERS substrates in 1979 by Creighton et al. [47], Au and Ag sols have been widely used as SERS substrates owing to their strong SERS activity. With the fast development of nanoscience and nanotechnology in the mid-1990s, the control of the shape, size, and composition of Ag and Au nanoparticles has become quite sophisticated. As a result, Ag and Au sols have become the most widely used SERS substrates. Theoretical calculations indicate that the Raman enhancement of a single Au nanoparticle is about 10^3–10^4, and that for a single Ag nanoparticle can reach about 10^6–

10^7 [53, 54]. Experimental results obtained with 647-nm excitation indicate that Ag nanoparticles with a diameter of about 200 nm and Au nanoparticles with a diameter of about 60 nm show the highest enhancement [55, 56]. Although spherical Au nanoparticles show surface plasmon resonance absorption at about 530 nm, the efficiency of inducing localized electromagnetic field enhancement is not high owing to the extension of the interband transition of Au into this wavelength region; therefore, reasonably good enhancement can only be obtained by using red excitation, typically 632.8 or 647 nm. Theoretical results have shown that metal nanoparticles with a sharp edge and angle will give an extra enhancement owing to the "lightning rod effect" [57, 58]. Experimental results also indicate that Au nanocubes or nanotriangles have a strong enhancement effect over nanospheres, among which the enhancement effect of nanocubes can be as high as 10^9 [59, 60], although in this finding one should not neglect the coupling effect of a Au substrate on enhancement. Most of the above-mentioned nanoparticles show surface plasmon resonance absorption in the visible region; however, to apply SERS to study biological samples or cells, it is better to choose excitation light in the near-infrared region. Owing to the weak absorption of the near-infrared light by tissue and the lower energy of the light, it can penetrate deeper into the tissue and effectively avoid the interference of fluorescence. As a result, there has been special interest in preparing SERS substrates with LSPR absorption in the near-infrared region in recent years [60]. Among various type of nanoparticles, Au nanorods have a very unique absorption in the near-infrared region. Different from the single absorption band of single spherical nanoparticles, nanorods show transverse and longitudinal LSPR modes due to the geometric asymmetry. The former occurs in the short-wavelength region and the latter occurs in the long-wavelength region, and usually the latter shows a stronger absorption than the former. The longitudinal band will redshift and increase in intensity with increasing aspect
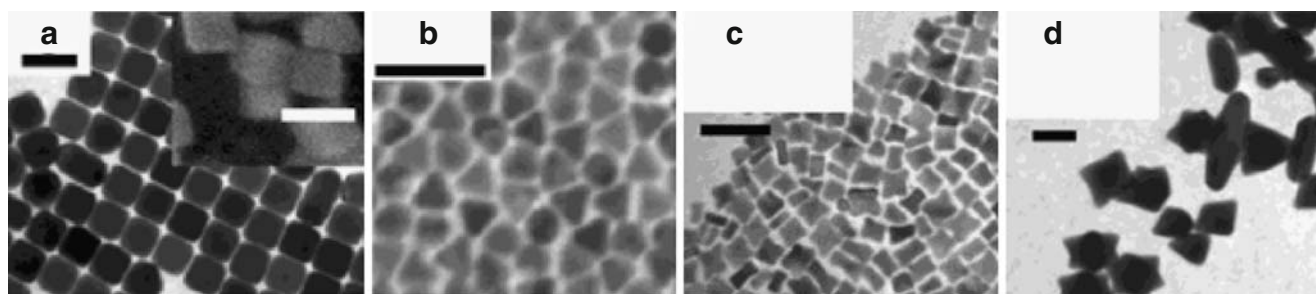
Fig. 1 Transmission electron microscopy images of Au nanoparticles synthesized under different conditions (*inset* scanning electron microscopy, SEM). The concentration of Au seed increases from **a** to **b**. The concentration ratio of seed to Au^{3+} and the concentrations of cetyl trimethylammonium bromide and ascorbic acid vary from **c** to **d**. *Scale bar* 100 nm. (Redrawn with permission from [50], copyright American Chemical Society)

ratio, which dominates the optical properties of nanoparticles [61]. For example, Au nanorods with an aspect ratio of 4 show an absorption band at about 800 nm. They are ideal substrates for 785-nm excitation and have been used for cancer cell detection [60]. However, owing to the isotropic feature of nanorods, the enhancement obtained from them may also depend very much on the direction of polarization of the light and the long axis of the nanorods, which may lead to some complications in using them as substrates.

Compared with the SERS effect of Au and Ag nanoparticles, that of transition metal nanoparticles is relatively weak. Transition metal nanoparticles are normally used for studying the electrocatalytic and corrosion processes of transition metals. The pioneering work on using transition metal nanoparticles as SERS substrates dates back to 1984, when Parker et al. [62] synthesized Rh sols and used them to detect the SERS of pyridine. It was not until 1997, after the demonstration that there is a SERS effect on transition metals [33, 63], that SERS was also observed on Pd [64], Fe [65], and Pt [66, 67] nanoparticles. Owing to the difficulty in synthesizing large transition metal nanoparticles, most of the previous studies were performed using small nanoparticles (less than 20 nm in diameter), and as a result the enhancement was usually weak. More recently, with use of a special capping agent, Pt nanocubes and Pd nanotriangles have been synthesized and used as SERS substrates. Both of them show higher enhancement than the respective spherical nanoparticles, possibly owing to the special effect of the sharp edge [68, 69]. To overcome the weak SERS activity of transition metal nanoparticles, we further coated the Au core with an optimized SERS activity with a very thin layer (one to ten atomic layers) of a transition metal shell (Pt, Pd, Ni, Co, etc.) and obtained Au core–transition metal shell nanoparticles. With the assistance of the long-range effect of the SERS of the Au core, the SERS of molecules adsorbed on transition metal shells can be significantly improved. The enhancement can be as high as 10^4–10^5 [70, 71]. Such core–shell nanoparticles have been used for studying the electrochemical process and interfacial structure [70–72].

Both experimental and theoretical results indicate that a stronger enhancement effect will be produced when the single nanoparticles form aggregates of two or multiple nanoparticles owing to the coupling of the electromagnetic field. For instance, in single-molecule SERS, enhancement as high as 10^{14} has been claimed [73, 74]. A high concentration of probe molecules or some salts (such as NaCl) will help to form aggregates in the sol and improve the SERS activity [51, 75]. It should be pointed out that in the multiple-nanoparticle system, the SERS enhancement will not only be influenced by the size, shape, and interparticle spacing, but also by the polarization of the laser. In such a system, the interparticle spacing and arrangement is random. Therefore, the experimentally obtained signal is the averaged spectra contributed by systems of different enhancements, which will lead to a poor reproducibility of the spectral intensity in the multiple-nanoparticle coupling system. Especially, the sol is usually stabilized by the surface charge or the steric hindrance of polymeric molecules on the nanoparticle surfaces. One would expect chemical degradation or aggregation of the nanoparticles in the sol owing to the change in surface charge or the desorption or decomposition of polymeric molecules. Furthermore, after the addition of sample molecules and salt, the nanoparticles may form precipitates after the formation of aggregates, which may lead to a significant decrease of the SERS signal in a few minutes [76]. Therefore, to obtain signals with very high reproducibility, it is better to use highly ordered substrates; these will be discussed later.

In comparison, the synthesis of well-dispersed single spherical nanoparticles with a size deviation of less than 10% is becoming very sophisticated. The spectral reproducibility is already good enough for quantitative analysis; however, owing to the weak enhancement, it is only applicable to some molecular systems with a strong Raman signal. Furthermore, in the single-particle SERS measurement, it is very important to keep the nanoparticles from aggregating and stabilized in the sol. For this purpose, the nanoparticle surface will usually be modified with charged molecules or molecules with a large steric hindrance effect. These molecules, on the other hand, will occupy some of the surface sites and prevent the direct adsorption of target molecules on the surface, which will also lead to a decrease of the SERS signal, especially when the target molecules do not have strong interaction with the substrate. Therefore, up to now, there is still limited use of sols for direct SERS detection. A more prevalent method of using SERS for quantitative analysis is to use an indirect detection method. Typically, a Raman marker with a very strong Raman signal (usually a molecule with a resonance Raman effect at the excitation wavelength) is adsorbed on the nanoparticle surface. Then the surface is further modified with an inert layer [SiO_2, thiol-modified poly(ethylene glycol), poly(acrylic acid) plus poly(allylamine hydrochloride), etc.] with a very weak Raman signal. Afterwards, some molecules that can specifically interact with the target molecules (antibody–antigen, biotin–avidin, aptamer–protein specific interaction) are linked to the inert layer. Finally, the modified nanoparticles can be use for indirect quantitative analysis of the target molecule by detecting the SERS signal of the Raman marker. A detailed scheme of the detection principles is shown in Fig. 2 [77–81]. Special attention has to be paid to the signal intensity by choosing the right nanoparticles and the right Raman marker and the unspecific interaction.

Fig. 2 Architectures used in surface enhanced Raman scattering (SERS) experiments using metal nanoparticles encapsulated in silica (*blue route*), polymer (*red route*), and polyelectrolytes (*green route*). *TEOS* tetraethyloxysilane, *APTMS* aminopropyl trimethoxysilane, *PAA* poly (acrylic acid), *PAH* poly(allylamine hydrochloride), *PEG-SH* thiol-modified poly (ethylene glycol)
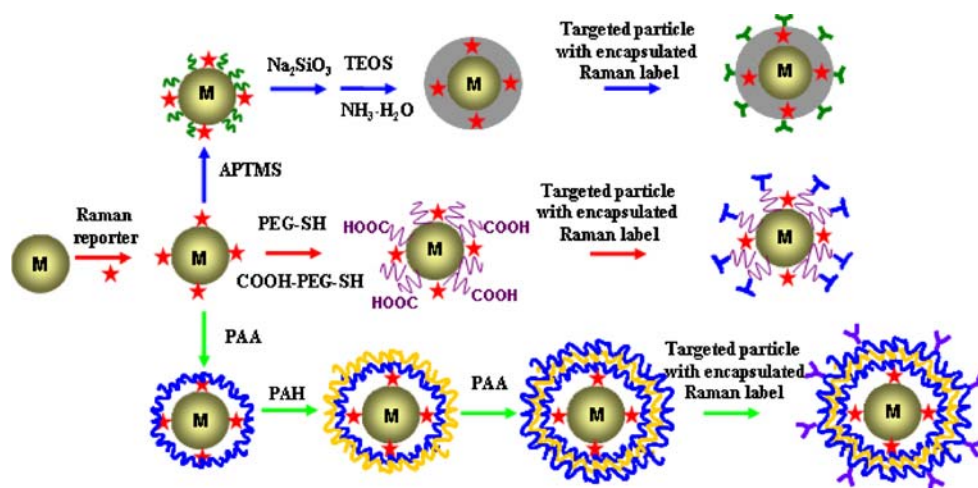
As mentioned above, the SERS signals obtained from the well-dispersed nanoparticle sols are usually very weak. Therefore, a more common method is to disperse the synthesized sol or sols that have been cleaned by centrifugation on a solid substrate (such as glass, Si, or metal surface) to form a compact layer of nanoparticles to effectively induce the coupling between nanoparticles. This method is very simple but provides very high enhancement, and has been widely adopted. It should be especially pointed out that to form a well-dispersed layer of nanoparticles the substrate has to be thoroughly cleaned to obtain a highly hydrophilic surface. Even so, the nanoparticle layer formed by a single dispersion is still very nonuniform and the SERS signals in different areas are quite inhomogeneous. A much more uniform SERS substrate can be obtained by concentrating the sol and by controlling the dropping times and drying rate (Fig. 3) [72]. The signal deviation in different areas of the substrate can be less than 10%. One should also realize that the surface layer will no longer be transparent and that it is hard to estimate the quantity of nanoparticles on the surface after several cycles of dropping and drying, which may limit to some

extent its application in the study of living cells, quantitative analysis, and the SERS enhancement effect. If it is possible to obtain a SERS substrate with a highly ordered monolayer, it will be of great significance to help understand the SERS mechanism, extend the application of SERS, and finally be recognized and accepted by the field of analytical sciences.

Highly ordered SERS substrates

The methods to prepare highly ordered SERS substrates include the nanoparticle assembly method, the Langmuir–Blodgett (LB) method, the template method, and nanolithography and nanoimprint methods. In the following part, the preparation method and the advantages and disadvantages will be analyzed for different methods.

Chemical assembly method

This method is to modify the solid substrate [Si, glass, indium tin oxide (ITO), or Au film] with a bifunctional molecule. The molecule forms a compact layer with the

Fig. 3 SEM images of nanoparticles dispersed on electrode surfaces as a SERS-active substrate: **a** Au nanospheres; **b** Au core–Pd shell nanocubes. (Redrawn with permission from [72], copyright Royal Society of Chemistry)
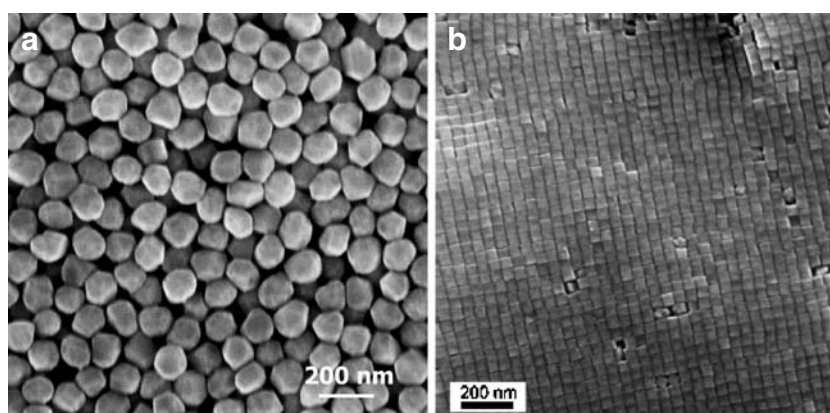
solid substrate with one moiety and another moiety interacts with the nanoparticles through electrostatic or chemical interaction to form an ordered layer of nanoparticles. Different bifunctional molecules should be selected for different substrates. For example, a molecule with SH and a N lone pair group can be selected for Au, Ag, Pt, and Pd substrates [82]. Special care should be taken for thiol, because thiol can be easily dimerized to form disulfur compounds and this leads to the annihilation of the functional group and a bad assembly effect. A Si or glass substrate should usually be completely degreased and activated to form a surface hydroxyl group, which can then react with the siloxane group of the bifunctional molecules [83]. The surface coverage and uniformity of the assembled layer depend primarily on the size, concentration, and surface charge of the nanoparticles, and the type of bifunctional molecules. During the synthesis process, capping agents are usually added to prevent the aggregation of nanoparticles and to form a uniform substrate. However, the presence of the capping agent will lead to a large repulsion between nanoparticles and prevent the formation of a compact assembly layer. As a result, the electromag-

netic coupling between nanoparticles cannot be highly effective and the SERS activity will be low [84]. To overcome this problem, further growth of the nanoparticles by chemical or electrochemical methods has been proposed to reduce the interparticle spacing and increase the SERS activity [85, 86] (Fig. 4). The advantage of the method is that it can tune the optical properties of the substrate by controlling the interparticle spacing. Although the arrangement of nanoparticles on the surface during the assembly process is still rather random, the signal is quite homogeneous over the whole surface because the laser spot covers a range of several microns containing several hundred nanoparticles and the resulting signal is an average of the signals from these nanoparticles. The most attractive advantage is that a substrate with a very homogeneous SERS signal and large area (up to several square centimeters) can be fabricated in a normal laboratory without complicated equipment.

An alternative method is to functionalize the Au nanoparticle surface with CTAB to form a positively charged molecular bilayer. Then a droplet of the functionalized nanoparticles is dispersed on a precleaned ITO glass surface

Fig. 4 a Preparation of a SERS-active substrate of Au nanoparticles on an indium tin oxide glass surface by combining the self-assembly and electrodeposition methods. b, c SEM images of the assembled substrate before and after electrodeposition. NPs nanoparticles
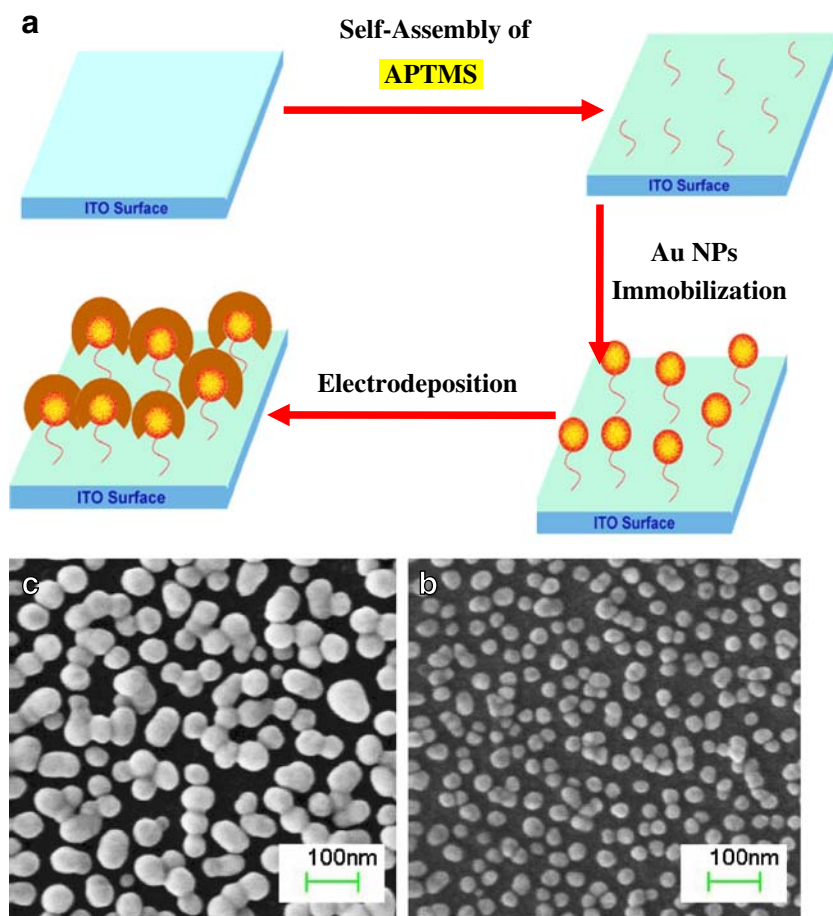
to form a very uniform layer of Au nanoparticles, with the interparticle spacing controlled by the length of the CTAB molecule (approximately 8 nm). Owing to the positive charge of the bilayer surrounding the nanoparticles, the nanoparticles will not form aggregates on the surface during the process of evaporation of the solvent. The small interparticle spacing enhances coupling between nanoparticles, which will lead to a shift of the LSPR of the substrate to the near-infrared region and a 10^8 enhancement [87]. The substrate has a very uniform SERS signal and good reproducibility and stability. It should be pointed out that even for a strongly adsorbed molecule such as p-mercaptoaniline, the signal of CTAB can still be detected. This will limit to some extent its application for detecting molecules with a weak interaction with the substrate or a weak Raman signal. The problem can be solved by a kind of surface cleaning method, as will be discussed later. Although this method can effectively avoid the aggregation of nanoparticles, it is still difficult to obtain a defect-free surface and to obtain a substrate with a large area. The LB technique can potentially solve this problem.

LB technique

The LB technique was originally used to prepare a large-area film of amphiphilic molecules on solid substrates [88]. By dissolving an amphiphilic molecule in a volatile solvent immiscible with water, and dispersing the solution on the surface of the water phase, a monolayer of the molecule will form at the interface after the evaporation of the solvent. By changing the position of the movable barrier in the LB trough, one can change the density of the monolayer film. The film can then be deposited on the substrate by the dipping and pulling method. Similarly, to prepare a nanoparticle film, the nanoparticles should first be modified with hydrophobic molecules and dispersed into highly volatile chloroform or hexane, which is immiscible with water. By dispersion of the solution into the water phase, a layer of randomly distributed nanoparticles will be left at the interface after the evaporation of the solvent. As a result of compression of the layer through moving the barrier, an ordered layer of nanoparticles will be formed on the surface [89]. A systematic study by the Yang group [29, 89–91] has demonstrated the promising future of this type of substrate for SERS. During the compression process, the interparticle spacing will decrease, leading to strong electromagnetic coupling between nanoparticles and a significant shift of the LSPR band. The obvious color change during the compression process clearly demonstrates the change. Under very high pressure, the nanoparticle film even presents a metallic luster. The film structures formed by different types of nanoparticles are quite different. For example, spherical and cubic nanoparticles can easily form

a highly ordered close-packed film, whereas nanorods or nanowires tend to align perpendicular to the compression direction and form a rather ordered structure in a large area and a less ordered structure in comparison with spherical nanoparticles in a small area. The formation of a liquid-crystal-like structure of the nanorod film makes it an ideal model to correlate the laser polarization with the LSPR and the SERS signal. The nanoparticle film can then be deposited on glass or a Si wafer by transfer to form a substrate with a surface area as large as 20 cm². At present, the LB technique has been successfully used to fabricate SERS films of nanorods, nanowires, and spherical, cubic, cuboctahedral, and octahedral Ag nanoparticles (Fig. 5) [89]. Among them, the Ag nanocube shows the lowest enhancement, and the octahedral nanoparticle shows the highest enhancement, up to $10^7–10^8$. With use of the latter as a SERS substrate, a detection limit as low as 1 ppb has been achieved for the detection of arsenate and arsenite in solution [29]. We should also note that similar to the above-mentioned CTAB-modified method, in the LB method, the nanoparticles should also be modified with some molecules that may also interfere with the SERS measurement. Nonetheless, the LB method is the method that is capable of achieving the most uniform substrate based on the nanoparticle assembly method. As Tao et al. [89] stated in their review: "It is most likely, however, that these techniques will not completely supersede top-down approaches but instead will provide a complementary tool for nanoscale patterning. The greatest advantage of the techniques presented here is that no specialized equipment is necessary."

Anodic aluminum oxide template method

The electrochemical oxidation of electrochemically polished Al foil under strictly controlled conditions will result in the formation of a two-dimensionally ordered anodic aluminum oxide (AAO) nanopore template. The diameter of the nanopores can be adjusted in the range of 15–150 nm by the oxidation voltage, the pH of the solution, and the reaction temperature during the oxidation process. Highly ordered nanowires or nanorods can be prepared by depositing metals into the nanopore using electroless, AC, or DC electroplating (Fig. 6). Electroless plating turns to be the simplest method by using $SnCl_2$ as a sensitizer and $PdCl_2$ as an activating agent and can be performed by dipping the template into the plating solution containing metal salt and reductants [92]. However, electroless plating usually starts from the bottom and the wall of the pore and tends to form nanotubes. It is also difficult to control the length and the crystallinity. AC electroplating is performed by dipping the template directly into the electroplating solution containing metal salt without removing the barrier

Fig. 5 SEM images of a monolayer of nanocrystals and nanowires prepared by the Langmuir–Blodgett technique: **a** Pt nanospheres; **b** Ag truncated nanocubes; **c** Ag nanowires; **d** Ag octahedral nanoparticles. (Reprinted with permission from [91], copyright 2007 Macmillan Publishers Ltd.)
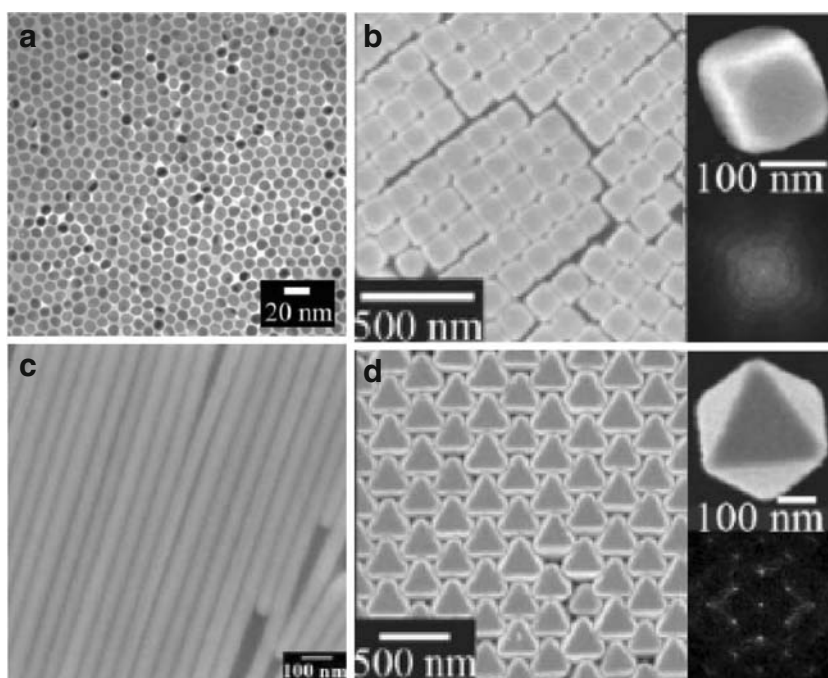

layer and the Al. The deposition voltage depends on the thickness of the barrier layer of the AAO template and varies from 2 to 20 V. In the AC electroplating method, the plating is limited inside the pore owing to the voltage regulation; therefore, the length of the metal nanowires is usually less than the thickness of the template. By dissolving part of the template in dilute H_3PO_4 solution, one can expose highly ordered metal nanowire arrays for SERS measurement [33, 93]. In the DC electroplating process, the barrier layer should be removed first before the electroplating, or a layer of conducting metal is deposited by vacuum methods on the AAO surface and then the Al layer and the barrier layer are removed for further electroplating. The DC electroplating method is rather complicated, but the nanowires obtained have good crystallinity [94]. In comparison with other methods for preparing SERS substrates, the AAO template method has the following advantages: the process is simple and highly reproducible and can be done at a low cost; the type of metal, the

diameter, and the length can all be controlled to request; the interwire spacing can be narrowed down to 10 nm or even 5 nm by a pore-widening technique [95, 96]; no surfactants or capping agents are needed during the fabrication process and therefore the substrate is very clean; it is easy to obtain an ordered plate up to a size of square centimeters. But at present, it is still a great challenge to obtain a gap of less than 5 nm owing to the corruption of the template at such a thin wall thickness.

Nanosphere lithography

Another type of ordered SERS substrate that has been shown to very promising is fabricated on the basis of the nanosphere lithography method, mainly through the efforts of the Van Duyne group [22] and the Bartlett group [97]. By assembly of polystyrene or silica spheres of desired size on a clean substrate (glass, ITO glass, Si or metal film), a monolayer or a multilayer of the highly ordered nanosphere

Fig. 6 **a** The fabrication processes of metal nanorod/nanowire arrays. **b** The atomic force microscopy image of Ni nanorod arrays after the anodic aluminum oxide layer had been partially removed in solution of 4% H_3PO_4
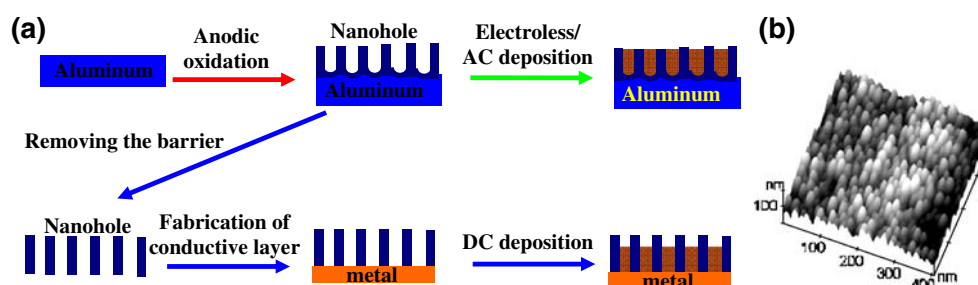
film will form on the substrate by controlling the assembly conditions. The film is then used as the template for vacuum deposition or electrochemical deposition to form on the template a metal film of the desired thickness. As a result, three kinds of structured SERS substrates may be produced (Fig. 7): (1) physical vapor deposition on the nanosphere template leads to the formation of a metal (e.g., Ag or Au) "film over nanosphere" (FON) surface; (2) removal of nanospheres in the FON substrate by sonicating the entire sample in a solvent results in surface-confined nanoparticles with a triangular footprint; (3) electrochemical deposition followed by removal of the nanosphere leaves a thin nanostructured film containing a regular hexagonal array of a uniform metal nanoisland, nanobowl to nanovoids depending on the thickness of the deposited film. The advantage of the nanosphere lithography method for preparing the SERS substrate is that the shape, size, and spacing of the nanostructures can be controlled by the size of the nanospheres and the thickness of the deposited metal so that the LSPR position can be adjusted to match the excitation wavelength and to achieve an optimized SERS enhancement [98]. Methods 1 and 3 will produce substrates with high SERS enhancement. Although the SERS activity of the second method is comparably low owing to the large spacing between particles, the outstanding LSPR tenability results in an excellent LSPR sensing chip. Although it is rather routine to obtain an ordered substrate with an area of 10–100 μm^2 in some experienced groups [99], the success rate of this method really depends on the experience of the experimentalist and how strictly the experimental conditions can be controlled. It is extremely challenging to obtain an ordered surface without any point or line defects when the size of the sphere is less than 200 nm. However, with the help of a microscope, it is still quite easy to find an ordered area for quantitative analysis with very good reproducibility and stability.

Nanolithography and nanoimprint

The ultimate method to obtain a highly ordered array is to use the top-down nanolithography and related nanoimprint methods. Typically, a layer of polymeric photoresist (positive or negative) is cast on the solid substrate (such as Si, glass, or Au film), followed by patterning with ultraviolet light, an electron beam, or a focused ion beam directly on the photoresist surface or indirectly with the assistance of a mold. After exposure and development, the remaining photoresist can be used as a mold, on which SERS-active metals are deposited by vacuum physical vapor deposition. After the mold has been lifted off, a highly ordered nanostructured SERS-active substrate with a structure identical or complementary to that of the mold is formed [100, 101]. In the case of a Au film substrate, the resist masks obtained can also be used as stencils for ion beam etching of the exposed Au substrate. Then, the residual polymeric photoresist can be dissolved to expose the SERS structures [102]. The nanolithography method allows the preparation of highly ordered and uniform SERS substrates with nanostructures having a wide diversity of shapes and geometries compared with nanosphere lithography. However, it is still a challenge to routinely obtain a spacing of less than 10 nm to allow the maximized electromagnetic coupling. The use of focused ion beam or electron beam lithography to make a SERS substrate of large area is still time-consuming and the cost

Fig. 7 Template methods using nanosphere lithography to fabricate ordered nanostructured SERS-active substrates. *PS* polystyrene. (Reprinted with permission from [72], copyright Royal Society of Chemistry)
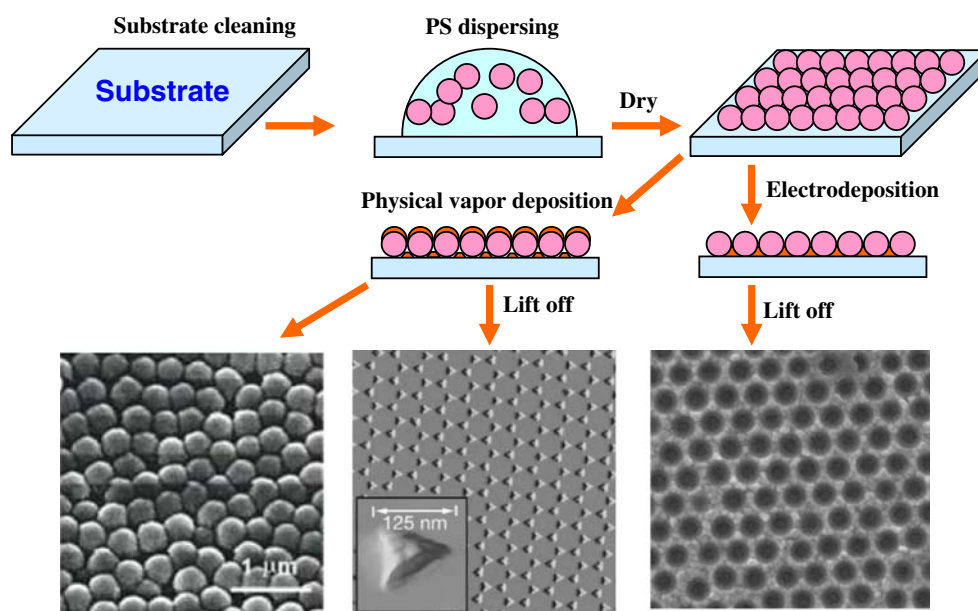
is too high for commercialization. Only those laboratories having the facilities are able to use them to fabricate SERS substrates for mechanistic study. Owing to the above-mentioned facts, these two methods will not be widely used because of the low efficiency and high cost. However, if the two methods are used to make molds to be used in nanoimprint, batch production will be possible. Nanoimprint normally directly writes on the Si or quartz slide with an electron beam to produce the desired nanopattern as the mold. The mold is then aligned and pressed into the photoresist covering on the substrate. After curing, the mold is lifted off and the substrate is deposited with the desired metal. After removal of the photoresist, a highly ordered nanostructure with SERS activity can be obtained [103]. Compared with nanolithography, nanoimprint has a much higher efficiency and lower cost. However, the problems associated with the mold, such as the weak coupling and low enhancement effect, still exist. Although there have been attempts to obtain the rough nanoarrays by changing the deposition conditions or posttreatment to increase the SERS activity of the fabricated nanostructures [104], such kinds of treatment will also lead to the problem of nonuniformity.
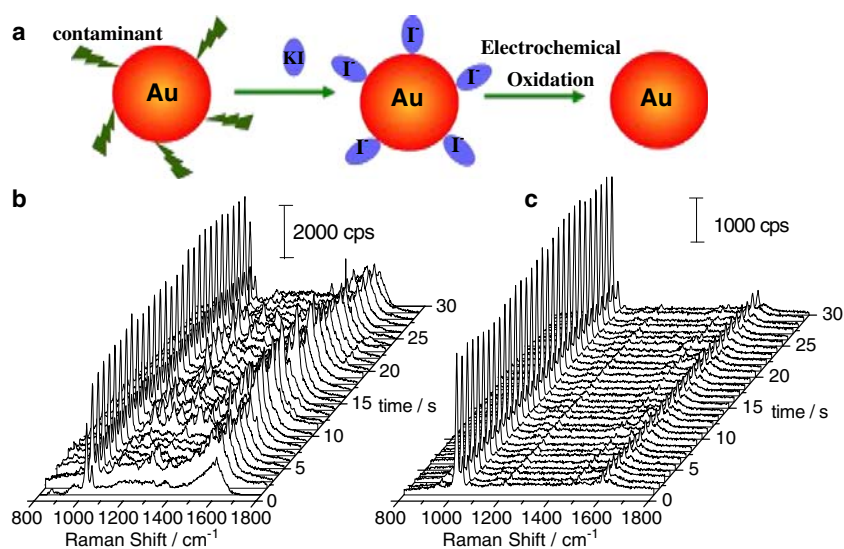
SERS substrate cleaning

Among various methods for fabricating SERS substrates as mentioned already, the reductants or surfactants (such as citrate, CTAB, or PVP) introduced during the synthesis process may interact strongly with the nanoparticles. Even for the substrate fabricated by template methods, some contaminants may also stay on the surface or be adsorbed from the air. In both cases, the surface sites will be occupied by the impurities. When the contaminated substrate is used for SERS measurement, the following two cases will be met:

1. If the target molecule has a strong interaction with the nanoparticle surface and the signal of the target molecule is strong, then the target molecule will probably replace the contaminants on the surface. In this case, the interference of the contaminants can be neglected.
2. If the interaction of the target molecule with the nanoparticle surface is weak or the signal is weak, then it is difficult for the target molecules to occupy the surface active site. Meanwhile, the existing signal of the contaminants will strongly interfere with the signal of the target molecules.

Especially when the substrate is used for detecting species with low concentration or biological samples, the requirement of a clean SERS substrate will be even higher because of the low surface coverage and the complexity of the biological environment.

Various attempts have been made to obtain clean SERS substrates. The simplest way to obtain a clean surface for chemically synthesized nanoparticles is to centrifuge the sol several times to remove the unreacted reductants and the surfactants. However, several cycles of centrifugation will lead to the aggregation or even precipitation of nanoparticles, and eventually lead to a decrease of the SERS signal. For a conductive SERS substrate, the electrochemical method can be used for cleaning. For instance, by application of a very negative potential, the surface adsorbate can be desorbed from the surface, resulting in a clean surface. To avoid the readsorption of impurities on the surface when the potential is moved to a positive value, it is recommended to perform the cleaning in a flow cell [105]. The simplest way is to clean the substrate in a vacuum with plasma or ultraviolet-light-generated ozone to decompose the organic impurities [106, 107]. This method is especially suitable for nonmetallic surfaces, such as a semiconductor or ITO, but is not suitable for a metal surface owing to the oxidation of the metal surface, especially Ag substrate, which will lead to an order of magnitude decrease (depending on the amount of contaminants and the exposure time). However, the cleaned substrate will be contaminated again when it is transferred from the vacuum to the ambient air [108]. The surface can also be cleaned using competitive chemical adsorption. The main concept is to replace the surface contaminants with a stronger adsorbate having less interference with the SERS measurement of the target molecule. For instance, CN^- was used to chemically remove layers of Ag to obtain a clean and fresh surface [109, 110]. Alkanethiols were also used to remove carbonaceous-species on SERS substrates [107]. Since the SERS signal of alkanethiols is weak and the bands of CN^- are away from the major bands of organic molecules, the treated substrates can be directly used for SERS detection. If the signal of the target molecules is also weak, then the preadsorbed species can be removed by exposing them to ozone, which results in a decrease in the enhancement owing to the oxidation. Chloride ion was also used to remove the contaminants on a SERS-active Ag mirror. But it was not stated how to remove the specifically adsorbed chloride ion from the surface for better interaction of the target molecules with the surface or to eliminate the interference of Cl^- with the adsorption of target molecules [111]. Recently, we developed a method to use iodide, an ion with a strong adsorption on Au and Ag, to remove the surface contaminants. The adsorbed iodide was then electrochemically oxidized to form the weakly adsorbed IO_3^- that can be easily cleaned by rinsing to obtain a clean substrate (Fig. 8a). As can be seen from Fig. 8b and c, the background existing in the uncleaned surface is obviously suppressed after cleaning. As the oxidation potential of Au is very close to that of I^-, the oxidation of I^- will lead to the partial dissolution of Au, which will result in a decrease of signal by

Fig. 8 **a** The cleaning process. **b**, **c** Time-dependent SERS signals of pyridine obtained at the same point of the substrate **b** before any treatment and **c** after treatment with iodide followed by electrochemical oxidation. (Redrawn with permission from [112], copyright American Chemical Society)

50% [112]. Substrate cleaning is the prerequisite to the SERS detection of the weakly adsorbed molecules and unknown sample. How to develop a simple and effective cleaning method while retaining the SERS activity is vitally important for wide application of SERS.

An approach to reliable SERS measurement by the defocusing method

A common experience of a SERS experimentalist with a micro Raman system is that the SERS signal will keep changing with time with the extended illumination under a laser power on the order of milliwatts, which is considered a very low laser power in the conventional Raman measurement. The main reason is due to the use of a microscope objective with a large numerical aperture (NA), through which the size of the laser spot on the sample becomes much smaller than that in the conventional macro Raman system [113]. With the same laser power on the sample, the laser power density of a confocal Raman microscope is typically about 3 orders of magnitude higher than that in the conventional Raman instruments. Such a power density may not be a problem for the study of nonabsorbing or very stable molecules or crystals; however, it will be a disaster for some organic molecules or biomolecules [114, 115]. Common strategies to reduce this effect are to lower the laser power or to use a movable sample [2, 18, 116].

Moving the sample requires a specially designed stable moving stage and will sometimes disturb the systems to be studied; therefore, the most frequently used method is to reduce the laser power. As we know, the Raman intensity is linearly proportional to the laser power; therefore, a decrease in the laser power will also lead to a proportional

decrease of the Raman intensity [2]. More recently, there has been increasing use of the line focusing method to expand the point focus to a line focus to match the slit. This method can significantly decrease the laser power density but retains a high signal collection efficiency [2]. Its application is still limited by the optical design in that not all instruments can be installed with a line focusing lens.

However, in the normal micro Raman system, if we slightly move the sample off focus, the laser power density will be reduced significantly owing to the rapid expansion of the laser spot size under an objective with a high NA. On the other hand, the collection efficiency is mainly determined by the confocal properties of a specific micro Raman system. Normalizing the laser power density with that under the ideal focus condition, we obtain a different laser power density for a×50 (NA 0.55) objective, shown by the x-axis in Fig. 9. By using Si(111) as the sample, we experimentally obtained the Raman intensity of the 520.6-cm^{-1} peak of Si under different
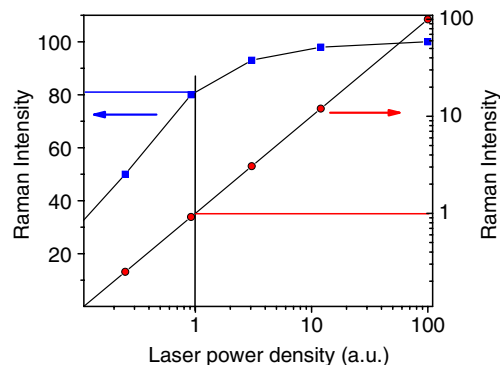
Fig. 9 The dependence of normalized Raman intensity on the laser power density obtained by the defocusing method (*left*) and by lowering the laser power (*right*)

off-focus conditions, and the result is shown by the left axis in Fig. 9 on a quasi-log scale. For comparison, the linear relation of the signal intensity with laser power is also shown (Fig. 9, right axis). From this figure, we can easily find that at the same laser power density of 1% of the original power density, the signal intensity retains over 80% of the original signal intensity with the defocusing method (by about 5 μm away from the focal plane), but the signal intensity decreases linearly to 1% on lowering the laser power. By defocusing about 25 μm away from the laser focal plane, one reduces the laser power density at the sample to about 0.043% of the ideal focus case; however, the Raman signal obtained still remains about 13% of the maximum signal. This result is extremely meaningful for those systems with a very weak Raman signal. Figure 10 demonstrates the striking effect of the defocusing method. The sample is a monolayer oligonucleotide-modified SERS-active Au surface. It can be seen from the figure that when the focus is about 20 μm away from the sample surface, the spectra are very stable and clean. However, at a distance of about 10 μm, the Raman intensity increases slightly, but the spectral features change with time and the Raman spectra also become slightly complicated. The situation becomes even worse when the sample surface is brought into the best focus. The spectra become noisy with a notable carbon background at around 1,600 cm^{-1} and those bands related to oligonucleotide disappear. It is quite obvious that the oligonucleotides have already decomposed under this high laser power density. It should be pointed out that all the spectra were obtained using the same acquisition time. We can easily conclude that a better focus did not always help improve the signal intensity or the signal-to-noise ratio because of the decomposition of
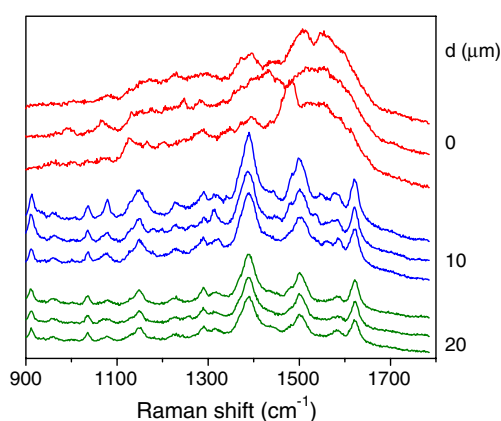
Fig. 10 The dependence of the surface-enhanced Raman spectra of an oligonucleotide-modified SERS-active Au surface on the defocusing distance of the sample to the ideal focal plane. The size of the confocal hole is 800 μm and the objective is a ×50 long working distance objective with a numerical aperture of 0.55. The laser power on the sample is 5 mW. All the spectra were obtained with 1-s acquisition time. The time delay in each set of spectra was roughly 1 s

the surface species, which produces the Raman and fluorescence signals giving the noisy background. The background deteriorates the Raman signal. This example convincingly proves that by using only the defocusing method, one can effectively lower the power density of the laser while collecting much stronger Raman signals than by lower power methods only. Apparently, a high NA objective will have a much more obvious effect and a large confocal hole size will improve the throughput and the Raman signal.

Evaluation of enhancement effect of SERS—calculation of surface enhancement factor

As mentioned already, different preparation methods will produce SERS substrates with unique advantages in a special application. The surface enhancement factor is an important indicator of the SERS activity of the substrate. With the application of SERS in single-molecule detection and in analytical sciences, different types of surface enhancement factors have been proposed, for example, single-molecule surface enhancement factor, analytical surface enhancement factor, and averaged surface enhancement factor (ASEF) [117]. The first of these is only related to the enhancement of a single molecule sitting at the special sites, such as a hot spot. Therefore, the enhancement is determined by the morphology of the substrates, the position of the probe molecule at the hot spot, the orientation of the molecules, as well as the polarization of the laser. It reflects the optical properties of the special surface site, which can be correlated with the theoretical result. The analytical surface enhancement factor is related to the SERS enhancement of analytes of known concentration. In this case, the signal intensity is the major concern and all the analytes are supposed to contribute to the final SERS signal. It neglects the fact that SERS is a kind of surface-sensitive phenomenon: only those molecules that are adsorbed at the surface feel the highest enhancement, and the enhancement decays exponentially with the increase of the distance to the surface. Therefore, it cannot reflect the real enhancement effect of the substrate. Apparently, these two kinds of enhancement factors reflect a special kind of enhancement effect and have no general applicability. Therefore, the ASEF that can really reflect the global enhancement of the substrate is more important [118–121]. The ASEF can be calculated by taking the ratio of the SERS signal contributed by a surface-adsorbed molecule to the normal Raman signal contributed by a molecule in solution or in the bulk:

$$\text{ASEF} = \frac{I_{\text{surf}}/N_{\text{surf}}}{I_{\text{bulk}}/N_{\text{bulk}}}, \tag{1}$$

where I_{surf} and I_{bulk} denote the integrated intensities for the strongest band of the surface and solution species, respectively, and N_{surf} and N_{bulk} represent the numbers of the corresponding surface and solution molecules effectively excited by the laser beam, respectively. In fact, there have been some erroneous calculations of the ASEF by overlooking some important values that need special consideration. There are two typical problems: (1) a resonance-enhanced molecule was used to calculate the ASEF; (2) the number of molecules in the laser spot was erroneously estimated, especially N_{bulk}. Therefore, we found it is still necessary to emphasize again how to reasonably estimate the enhancement factor and how to reasonably design the experiment to correctly obtain the experimental data for calculation of the enhancement effect.

In Eq. 1, I_{surf} and I_{bulk} can be directly obtained by integrating over the Raman spectra obtained. But for a molecule with a resonance Raman effect, the absorption spectrum may change after its adsorption on the surface owing to a change in the dielectric environment and the redistribution of electrons. It may lead to the move-in or move-out of the resonance wavelength, and may thus result in the overestimation or underestimation of the enhancement effect, respectively. To exclude such an obvious influence of the surface-bonding effect, it is better to use a nonresonance molecule as the probe molecule. N_{surf} can be calculated from the known surface area (A) by taking into account the surface roughness (R) in the illuminating spot and the surface area (σ) occupied by a molecule by assuming a full monolayer adsorption:

$$N_{surf} = \frac{RA}{\sigma}. \qquad (2)$$

If the coverage of the molecule is less than a monolayer, the ASEF will be underestimated. N_{surf} can be estimated more accurately by limiting the number of molecules to be slightly less than the number in monolayer during adsorption.

In the estimation of the ASEF, the greatest discrepancy occurs in the estimation of N_{bulk} owing to the special configuration of a confocal Raman microscope. The calculation methods for different types of systems, such as pure liquid, solution, pure transparent solid, and powder, will be different. Here we introduce the method developed by our group for the confocal Raman system to calculate N_{bulk}. When a laser beam is focused by an objective into the solution, a laser beam waist will be formed (Fig. 11a). In principle, all molecules within the illuminated volume of the solution can generate a Raman signal. The molecules in the focal plane contribute the most to the overall intensity and the contribution decreases dramatically from the molecules in the plane with increasing distance (z) to the ideal focal plane ($z=0$) (Fig. 11b). To estimate the number of molecules contributing to the total signal of solution

species, we proposed a method that involves immersing a single-crystal Si wafer in a solution in the cell with exactly the same setup as that used in surface Raman measurement. Then, the integrated intensity of the strongest band for Si at 520.6 cm^{-1} was measured while the Si wafer was moved through the illuminated volume, and the values obtained were plotted against z (Fig. 11b, solid line). This plot is considered to be the confocal depth profile under the real measuring condition. Experimentally, the solution spectrum is collected from the illuminated volume of the solution and is the sum of the signals from all the illuminated planes of the solution, just like the surface of a moving Si wafer, giving the same profile as that of the modeled Si wafer. It can be seen that the contribution to N_{bulk} from molecules outside the region $|z|>75$ μm is negligible. Now, assume an ultrathin layer of solution with a thickness of h and volume hA in the vicinity of the ideally focused plane, in which all the molecules have the same contribution to the overall signal as that in the ideal focal plane; the overall signal can be obtained by integrating the signal over the intensity profile. Thus, the thickness h can be calculated by

$$h = \frac{\int_{-\infty}^{\infty} I(z)\mathrm{d}z}{\mathrm{Im}\,\alpha x}. \qquad (3)$$

The h value (in micrometers) depends on the pinhole size and the objective lens of the Raman microscope. It should be especially emphasized that the h value can be significantly different in the cases with and without a quartz window and a solution layer. Therefore, in the experiment, the optical configuration for detecting SERS and normal Raman signals should be exactly the same, including the
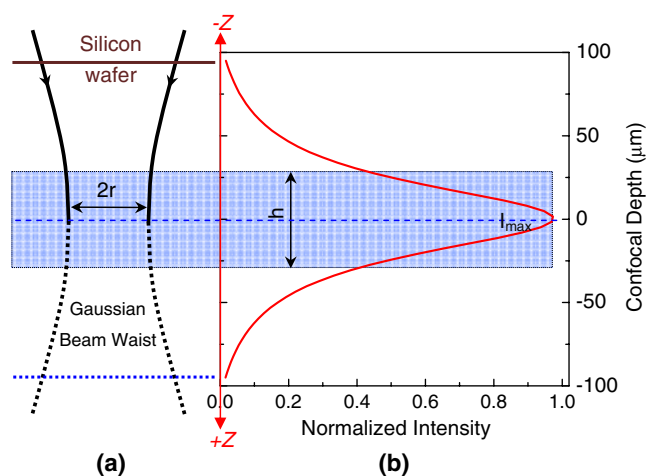
Fig. 11 **a** Waist profile of a laser beam in a solution and **b** the corresponding confocal depth (z) and intensity (I) profile of a moving Si wafer in an aqueous solution, simulating the collection volume of a solution spectrum. (Reprinted with permission from [36], copyright Springer)

window and the same thickness of the solution layer, if it is an electrochemical in situ measurement. However, if the surface Raman measurement is done in air, no window or solution layer is necessary. Now, the effective number of molecules contributing to the Raman signal will be

$$N_{bulk} = AhcN_A, \tag{4}$$

where c is the concentration of adsorbate in solution and N_A is the Avogadro constant. With Eqs. 2 and 4, Eq. 1 can be rearranged as

$$ASEF = \frac{I_{surf} cN A\sigma h}{I_{bulk} R}. \tag{5}$$

The ASEF can be obtained after substituting all the known data and constants into Eq. 5. The roughness factor R can be estimated by calculating the surface area using a simple sphere model for monolayer-dispersed nanoparticles. However, for multilayer nanoparticles or massive electrode surfaces, it is better to use electrochemical methods, such as differential capacitance or cyclic-voltammetric methods to estimate R. σ is generally obtained from the literature from previous studies and can also be estimated from known atom sizes and bond distances. The latter may often lead to an underestimation of σ and the ASEF value [12, 13, 43–48]. The advantage of using this method is that the value is not directly related to the area of the laser spot, as the area can be removed by taking the ratio, eliminating possible error. If the solution can be confined to a very thin layer with known thickness of less than 10 μm, we can still use Eq. 5. But the calculation becomes simple by substituting the h value with the known thickness of the solution layer.

A second method to calculate N_{bulk} is to confine the pure liquid of the probe molecules into a thin layer film, or by spin-coating the saturated solution of solid probe molecules on a smooth substrate to form a thin film of known thickness, h. Then, N_{bulk} can be easily calculated by

$$N_{bulk} = \frac{Ah\rho}{m} N_A, \tag{6}$$

where h is the thickness of the film or liquid layer, ρ is the density of the pure sample, and m is the molecular weight of the probe molecule.

By substituting Eqs. 2 and 6 into Eq. 1, one can obtain the ASEF as

$$ASEF = \frac{I_{surf} h\rho N_A}{I_{bulk} Rm}. \tag{7}$$

It is advised to make the thickness less than 10 μm for a transparent liquid sample to avoid the overestimation of the numbers. For the solid sample, the film thickness can be prepared to less than 1 μm to avoid the interference due to the absorption of the solid sample. The film thickness can be calibrated by optical methods or by scanning electron microscopy. It is recommended that a SERS laboratory prepare such a type of standard sample to be used as a reference standard for calculating the surface enhancement factor. Only when there is an accepted method to be used by different groups can the surface enhancement effects of different substrates be compared.

Conclusion

Different methods have been introduced to fabricate SERS substrates, including EC-ORC, vacuum deposition methods, well-dispersed nanoparticle sols, nanoparticle aggregate film surfaces, and well-ordered substrates. The advantages and disadvantages of different substrates in terms of application have been analyzed and proper fabrication methods should be selected for a special purpose of SERS. The well-dispersed nanoparticles show a weak but a homogenous enhancement. The spectral reproducibility of the nanoparticle aggregates or an electrochemically fabricated substrate is bad but very strong enhancement can be achieved by controlling the experimental conditions. Highly ordered substrates show excellent surface uniformity, but with a lower enhancement effect than nanoparticle aggregates. In short, each method has its advantages and weaknesses. Therefore, one should choose the right method to obtain a SERS-active substrate for a specific application. Well-dispersed nanoparticles and well-ordered substrates can be used for quantitative analysis. The nanoparticle aggregates can be effectively used for qualitative analysis with extremely high sensitivity.

Different methods to obtain clean SERS substrates have been analyzed and a method of iodide adsorption to repel the surface contaminants followed by the electrochemical oxidation method of iodide has been proposed. The method has been demonstrated to be useful for SERS detection of weak adsorbates and for trace analysis.

A defocusing method was proposed to effectively eliminate the laser-induced photodecomposition of surface adsorbate at the high laser power density of a micro Raman system. A 20-μm deviation of the laser focus from the sample surface can effectively eliminate the decomposition evidenced by the spectra free of carbonaceous background. Whether the substrate should be cleaned and how to clean it really depends on the systems to be measured. It is a great challenge to obtain a clean substrate with high enhancement, good uniformity, high reproducibility, and high stability.

Some existing problems in calculating the surface enhancement factor were discussed and a method to calculate the ASEF was introduced to allow the SERS activities of substrates prepared by different methods to be compared.

It is believed that the rapid development of nanoscience and nanotechnology will accelerate the process toward this goal, which will eventually allow a complete understanding of the SERS effect and a wide application of SERS in analytical science and biomedical sciences.

References

1. Pettinger B (1992) In: Lipkowski J, Ross PN (eds) Adsorption of molecules at metal electrodes. VCH, New York, pp 285–345
2. McCreery RL (2000) Raman spectroscopy for chemical analysis. Wiley-Interscience, New York
3. Smith E, Dent G (2005) Modern Raman spectroscopy. Wiley, New York
4. Hartschuh A (2008) Angew Chem Int Ed 47:8178–8191
5. Fleischmann M, Hendra PJ, Mcquillan AJ (1974) Chem Phys Lett 26:163–166
6. Jeanmaire DL, Van Duyne RP (1977) J Electroanal Chem 84:1–20
7. Albrecht MG, Creighton JA (1977) J Am Chem Soc 99:5215–5217
8. Tian ZQ (ed) (2005) Journal Raman Spectrosc 36:465–747
9. Brown R, Milton MJT, Smith WE (eds) (2006) Faraday Discuss 132:1–340
10. Graham D, Goodacre R (eds) (2008) Chem Soc Rev 37:873–1076
11. Furtak TE, Chang RK (1982) Surface enhanced Raman scattering. Plenum, New York
12. Otto A, Mrozek I, Grabhorn H, Akemann W (1992) J Phys Condens Matter 4:1143–1212
13. Moskovits M (2005) J Raman Spectrosc 36:485–496
14. Tian ZQ (2006) Faraday Discuss 132:227–247
15. Ding SY, Wu DY, Yang ZL, Ren B, Xu X, Tian ZQ (2008) Chem J Chin Univ Chin 29:2569–2581
16. Gersten JI, Birke RL, Lombardi JR (1979) Phys Rev Lett 43:147–150
17. Burstein E, Chen YJ, Chen CY, Lundquist S, Tosatti E (1979) Solid State Commun 29:567–570
18. Otto A (1984) In: Cardona M, Guntherodt G (eds) Light scattering in solids. Springer, Berlin, pp 289–418
19. Moskovits M (1985) Rev Mod Phys 57:783–828
20. Gersten JI (1980) J Chem Phys 73:3023–3037
21. Hulteen JC, Van Duynea RP (1995) J Vac Sci Technol A 13:1553–1558
22. Willets KA, Van Duyne RP (2007) Annu Rev Phys Chem 58:267–297
23. Natan MJ (2006) Faraday Discuss 132:321–328
24. Ackermann KR, Henkel T, Popp J (2007) Chemphyschem 8:2665–2670
25. Bell SEJ, Sirimuthu NMS (2008) Chem Soc Rev 37:1012–1024
26. Jarvis RM, Johnson HE, Olembe E, Panneerselvam A, Malik MA, Afzaal M, O'Brien P, Goodacre R (2008) Analyst 133:1449–1452
27. Shanmukh S, Jones L, Driskell J, Zhao YP, Dluhy R, Tripp RA (2006) Nano Lett 6:2630–2636
28. Kneipp J, Kneipp H, Kneipp K (2008) Chem Soc Rev 37:1052–1060
29. Mulvihill M, Tao A, Benjauthrit K, Arnold J, Yang P (2008) Angew Chem Int Ed 47:6456–6460
30. Evanoff DD, Heckel J, Caldwell TP, Christensen KA, Chumanov G (2006) J Am Chem Soc 128:12618–12619
31. Jarvis RM, Law N, Shadi LT, O'Brien P, Lloyd JR, Goodacre R (2008) Anal Chem 80:6741–6746
32. Qian XM, Zhou X, Nie SM (2008) J Am Chem Soc 130:14934–14935
33. Tian ZQ, Ren B, Wu DY (2002) J Phys Chem B 106:9463–9483
34. Tian ZQ, Ren B (2003) In: Bard AJ, Stratmann M, Unwin PR (eds) Encyclopedia of electrochemistry, vol 3. Wiley-VCH, New York, pp 572–659
35. Gao P, Weaver MJ (1985) J Phys Chem 89:5040–5070
36. Ren B, Liu GK, Lian XB, Yang ZL, Tian ZQ (2007) Anal Bioanal Chem 388:29–45
37. Fleischmann M, Tian ZQ, Li LJ (1987) J Electroanal Chem 217:397–410
38. Wing L, Leung H, Weaver MJ (1987) J Am Chem Soc 109:5113–5119
39. Weaver MJ, Zou SZ, Chan HYH (2000) Anal Chem 72:38A–47A
40. Rowe JE, Shank CW, Zwemer DA, Murray CA (1980) Phys Rev Lett 44:1770–1773
41. Moskovits M (1983) Chem Phys Lett 98:498–502
42. Knight DS, Weimer R, Pilione L, White WB (1990) Appl Phys Lett 56:1320–1322
43. Eickmans J, Otto A, Goldmann A (1986) Surf Sci 171:415–441
44. Taylor CE, Pemberton JE, Goodman GG, Schoenfisch MH (1999) Appl Spectrosc 53:1212–1221
45. Pileni MP (2007) J Phys Chem C 111:9019–9038
46. Frens G (1973) Nat Phys Sci 241:20–22
47. Creighton JA, Blatchford CG, Albrecht MG (1979) J Chem Soc Faraday Trans 75:790–798
48. Ahmadi TS, Wang ZL, Green TC, Henglein A, El-Sayed MA (1996) Science 272:1924–1925
49. Sun YG, Xia YN (2002) Science 298:2176–2179
50. Sau TK, Murphy CJ (2004) J Am Chem Soc 126:8648–8649
51. Kneipp K, Wang Y, Kneipp H, Perelman LT, Itzkan I, Dasari R, Feld MS (1997) Phys Rev Lett 78:1667–1670
52. Nie SM, Emory SR (1997) Science 275:1102–1106
53. Wang DS, Chew H, Kerker M (1980) Appl Opt 19:2256–2257
54. Kerker M (1987) J Colloid Interface Sci 118:1
55. Emery SR, Haskins WE, Nie SM (1998) J Am Chem Soc 120:8009–8010
56. Krug JT, Wang GD, Emory SR, Nie SM (1999) J Am Chem Soc 121:9208–9214
57. Gersten JI (1980) J Chem Phys 72:5779–5780
58. Kelly KL, Coronado E, Zhao LL, Schatz GC (2003) J Phys Chem B 107:668–677
59. Orendorff CJ, Gole A, Sau TK, Murphy CJ (2005) Anal Chem 77:3261–3266
60. Huang XH, El-Sayed IH, Qian W, El-Sayed MA (2007) Nano Lett 7:1591–1597
61. Link S, Mohamed MB, El-Sayed MA (1999) J Phys Chem B 103:3073–3077
62. Parker WL, Hexter RM, Siedle AR (1984) Chem Phys Lett 107:96–98
63. Tian ZQ, Ren B, Mao BW (1997) J Phys Chem B 101:1338–1346
64. Srnova I, Vlckova B, Baumruk V (1997) J Mol Struct 410–411:201–203
65. Guo L, Huang QJ, Li XY, Yang SH (2001) Phys Chem Chem Phys 3:1661–1665
66. Gomez R, Perez JM, Solla-Gullon J, Montiel V, Aldaz A (2004) J Phys Chem B 108:9943–9949
67. Kim NH, Kim K (2004) Chem Phys Lett 393:478–482
68. Cui L, Wang A, Wu DY, Ren B, Tian ZQ (2008) J Phys Chem C 112:17618–17624
69. Xiong YJ, McLellan JM, Chen JY, Yin YD, Li ZY, Xia YN (2005) J Am Chem Soc 127:17118–17127

70. Tian ZQ, Ren B, Li JF, Yang ZL (2007) Chem Commun 3514–3534
71. Tian ZQ, Yang ZL, Ren B, Li JF, Zhang Y, Lin XF, Hu JW, Wu DY (2006) Faraday Discuss 132:159–170
72. Wu DY, Li JF, Ren B, Tian ZQ (2008) Chem Soc Rev 37:1025–1041
73. Kneipp K, Kneipp H, Kartha VB, Manoharan R, Deinum G, Itzkan I, Dasari RR, Feld MS (1998) Phys Rev E 57:R6281–R6284
74. Kneipp K, Kneipp H, Manoharan R, Hanlon EB, Itzkan I, Dasari RR, Feld MS (1998) Appl Spectrosc 52:1493–1497
75. Keating CD, Kovaleski KM, Natan MJ (1998) J Phys Chem B 102:9404–9413
76. Bell SEJ, Sirimuthu NMS (2004) Analyst 129:1032–1036
77. Mulvaney SP, Musick MD, Keating CD, Natan MJ (2003) Langmuir 19:4784–4790
78. Qian XM, Nie SM (2008) Chem Soc Rev 37:912–920
79. McCabe AF, Eliasson C, Prasath RA, Hernandez-Santana A, Stevenson L, Apple I, Cormack PAG, Graham D, Smith WE, Corish P, Lipscomb SJ, Holland ER, Prince PD (2006) Faraday Discuss 132:303–308
80. Cui Y, Ren B, Yao JL, Gu RA, Tian ZQ (2006) J Phys Chem B 110:4002–4006
81. Kim K, Lee HB, Shin KS (2008) Langmuir 24:5893–5898
82. Freeman RG, Grabar KC, Allison KJ, Bright RM, Davis JA, Guthrie AP, Hommer MB, Jackson MA, Smith PC, Walter DG, Natan MJ (1995) Science 267:1627–1632
83. Grabar KC, Freeman RG, Hommer MB, Natan MJ (1995) Anal Chem 67:735–743
84. Grabar KC, Smith PC, Musick MD, Davis JA, Walter DG, Jackson MA, Guthrie AP, Natan MJ (1996) J Am Chem Soc 118:1148–1153
85. Brown KR, Natan MJ (1998) Langmuir 14:726–728
86. Gao MX, Lin XM, Ren B (2008) Chem J Chin Univ Chin 29:959–962
87. Wang H, Levin CS, Halas NJ (2005) J Am Chem Soc 127:14992–14993
88. Roberts G (1990) Langmuir Blodgett films. Plenum, New York
89. Tao AR, Huang JX, Yang PD (2008) Acc Chem Res 41:1662–1673
90. Tao A, Kim F, Hess C, Goldberger J, He RR, Sun YG, Xia YN, Yang PD (2003) Nano Lett 3:1229–1233
91. Tao A, Sinsermsuksakul P, Yang P (2007) Nat Nanotechnol 2:435–440
92. Menon VP, Martin CR (1995) Anal Chem 67:1920–1928
93. Yao JL, Tang J, Wu DY, Sun DM, Xue KH, Ren B, Mao BW, Tian ZQ (2002) Surf Sci 514:108–116
94. Zhai XF, Mu C, Xu DS, Tong LM, Zhu T, Du WM (2008) Spectrosc Spectral Anal 28:2329–2332
95. Lee SJ, Guan ZQ, Xu HX, Moskovits M (2007) J Phys Chem C 111:17985–17988
96. Wang HH, Liu CY, Wu SB, Liu NW, Peng CY, Chan TH, Hsu CF, Wang JK, Wang YL (2006) Adv Mater 18:491–495
97. Mahajan S, Abdelsalam M, Suguwara Y, Cintra S, Russell A, Baumberg J, Bartlett P (2007) Phys Chem Chem Phys 9:104–109
98. Haynes CL, Van Duyne RP (2003) J Phys Chem B 107:7426–7433
99. Dieringer JA, McFarland AD, Shah NC, Stuart DA, Whitney AV, Yonzon CR, Young MA, Zhang XY, Van Duyne RP (2006) Faraday Discuss 132:9–26
100. Gunnarsson L, Bjerneld EJ, Xu H, Petronis S, Kasemo B, Kall M (2001) Appl Phys Lett 78:802–804
101. Marquestaut N, Martin A, Talaga D, Servant L, Ravaine S, Reculusa S, Bassani DM, Gillies E, Lagugne-Labarthet F (2008) Langmuir 24:11313–11321
102. Huebner U, Boucher R, Schneidewind H, Cialla D, Popp J (2008) Microelectron Eng 85:1792–1794
103. Alvarez-Puebla R, Cui B, Bravo-Vasquez JP, Veres T, Fenniri H (2007) J Phys Chem C 111:6720–6723
104. Li ZY, Tong WM, Stickle WF, Neiman DL, Williams RS, Hunter LL, Talin AA, Li D, Brueck SRJ (2007) Langmuir 23:5135–5138
105. Zou SZ, Chen YX, Mao BW, Ren B, Tian ZQ (1997) J Electroanal Chem 424:19–24
106. Norrod KL, Rowlen KL (1998) Anal Chem 70:4218–4221
107. Norrod KL, Rowlen KL (1998) J Am Chem Soc 120:2656–2657
108. Taylor CE, Garvey SD, Pemberton JE (1996) Anal Chem 68:2401–2408
109. Bewicka A, Thomasa B (1975) J Electroanal Chem 65:911–931
110. Otto A (1978) Surf Sci 75:L392–L396
111. Cai ZP, Wang B, He TC, Zhang L, Mo YJ (2007) J Light Scattering 19:124–127
112. Li MD, Cui Y, Gao MX, Luo J, Ren B, Tian ZQ (2008) Anal Chem 80:5118–5125
113. Meinhart CD, Wereley ST (2003) Meas Sci Technol 14:1047–1053
114. Mahoney MR, Cooney RP (1983) J Phys Chem 87:5314–5319
115. Ramsey J, Ranganathan S, McCreery RL, Zhao J (2001) Appl Spectrosc 55:767–773
116. Vess TM, Wertz DW (1991) J Electroanal Chem 313:81–94
117. Le Ru EC, Blackie E, Meyer M, Etchegoin PG (2007) J Phys Chem C 111:13794–13803
118. Cai WB, Ren B, Li XQ, She CX, Liu FM, Cai XW, Tian ZQ (1998) Surf Sci 406:9–22
119. Felidj N, Aubard J, Levi G, Krenn JR, Salerno M, Schider G, Lamprecht B, Leitner A, Aussenegg FR (2002) Phys Rev B 65:9
120. McFarland AD, Young MA, Dieringer JA, Van Duyne RP (2005) J Phys Chem B 109:11279–11285
121. Hildebrandt P, Stockburger M (1984) J Phys Chem 88:5935–5944